Research Article

Degradation of Malachite green using heterogeneous nanophotocatalysts (NiO/TiO_2, CuO/TiO_2) under solar and microwave irradiation

Chafia Djebbari[1] · Emna zouaoui[2] · Nesrine Ammouchi[1,3] · Chafika Nakib[2] · Daoiya Zouied[2] · Karima Dob[1]

Received: 6 August 2020 / Accepted: 20 January 2021 / Published online: 2 February 2021

Abstract
Heterogeneous photocatalysis is an advanced oxidation process (AOP). This technique is used to degrade a wide range of pollutants in water. In this study, photocatalytic oxidation and mineralization of malachite green in an aqueous suspension containing nickel-based catalysts and copper supported on TiO_2 prepared by wet diffusional impregnation was studied using two sources of irradiation: solar and microwave. Photodegradation kinetics were studied according to several parameters, such as catalyst type, dye concentration, photocatalyst mass and microwave power. The results showed that the photodegradation of malachite green is faster in the presence of CuO/TiO_2 catalyst than NiO/TiO_2 catalyst than TiO_2. Dye degradation by microwave irradiation is faster than that by solar irradiation.

Keywords Photocatalysis · Pollutants · Supported catalyst · Photo degradation

1 Introduction

Several industries such as the textile, plastic paper, leather, pharmaceutical, cosmetic and nutrition use organic dyes (soluble or pigmented), to color their products and discharge their wastewater, into the environment without any previous treatment [8, 20].These colored effluents pose a serious risk to human health and aquatic environments [9, 10].

The most used methods for the treatment of the industrial wastewaters including biological and physico-chemical treatments, which in most cases cannot be sufficient to completely eliminate the organic load contained in these effluents [1]. To resolve these problems, new techniques were then developed to oxidize non-biodegradable organic compounds. Among the innovative techniques are advanced oxidation processes based on the production and use of a highly reactive and non-selective oxidant (the radical hydroxyl $HO^{\cdot}$) to mineralize partially or completely organic pollutants [3, 7, 11], Zhang and Deng 2011, [4]

The use of catalysts improves the performance and reduces the cost of these technologies, leading to more efficient removal of pollutants and more selective use of the oxidizing agent [19, 24]

The degradation process consists of a succession of radical oxidation initiated by strong oxidants such as $OH^{\cdot}$. $OH^{\cdot}$ are directly generated by the photolysis of water molecules adsorbed on the active sites of the catalysts. The organic pollutants adsorbed on the catalyst are then degraded by successive radical reactions into non-toxic mineral species [22]

TiO_2 is the most commonly used catalyst in advanced oxidation processes [17, 26]

The interest in TiO_2 is mainly due to its low-cost, non-toxicity chemical stability. However, TiO_2 with his large band gap absorbs photons in UV region which represent

✉ Emna zouaoui, zouaoui_amna@yahoo.fr | [1]Département de Sciences Technologiques, Faculté de Technologie, Université 20 Août 1955, Skikda, Algeria. [2]Département de Pétrochimie et Génie des Procédés, Faculté de Technologie, Université 20 Août 1955, Skikda, Algeria. [3]Laboratoire de physico-chimie, de surfaces et interfaces, Facultés de Technologies, Université 20 Août 1955, Skikda, Algeria.

5% of the solar spectrum. Thus, the rate of photocatalytic activity of TiO_2 is limited to the recombination rate of photoproduced electron–hole. To enhance the utilization of solar light for photocatalytic and to reduce electron–hole recombination, TiO_2 is modified by various metallic species and coupling with other semi-conductors [12, 13]

Many photocatalys is studies have been published using TiO_2 and doped TiO_2 as heterogeneous catalysts for the degradation of various organic pollutants [14, 15, 23].

The multiplex compound of TiO_2 with oxide sis one of the most effective methods for enhancing the photocatalyticactivity of modified TiO_2 (Pengwei et al. 2010). Several studies have indicated that oxide as a modifier can effectively increase the photocatalystactivity.

Zhang et al. prepared the SeO/TiO_2 nanocomposite, in which they proved that the recombination of electron–hole pairs has been effectively suppressed due to the formation of heterostructure and absorption has been extended to visible light due to the narrow band gap of 2.0 eV of Se^0 by the reduction of Se^{4+}(Zhang et al. 2007).

Tada et al. have shown that TiO_2 surfaces modified with iron oxide display visible light photocatalytic activity. The presence of iron oxide at the TiO_2 surface leads to charge separation, which is the origin of enhanced photocatalytic efficiency. Surface modification of a metaloxideisthus an interesting route in the development of visible light photocatalytic materials (Tada et al. 2011).

Arana et al. studiedmethyltert-butylether (MTBE) photocatalyticoxidationon CuO-Ti O_2 under UV irradiation. They observed a significant improvement of photocatalyticactivity of copper-modified titania in comparison with pure TiO_2 (Arana et al. 2017).

The aim of the present work is to synthesize two composite semiconductors based on nickel and copper supported on titanium dioxide (TiO_2) in order to increase its photocatalytic activity and investing their efficiency in the degradation of Malachite Green using sunlight and microwave irradiation.

2 Materials and methods

Materials used in this research were:

Malachite green (Aldrich).
Titanium dioxide (Merck).
Nickel nitrate (Merck).
Copper nitrate (Aldrich).
Hydrogen peroxide (Merck).

2.1 Preparation of catalysis

We impregnation method was used to prepare supported catalysts. The suspension of pure TiO_2 powder in a distilated water was mixed with the required amount of the nitrate copper nitrate trihydrate and nickel nitrate trihydrate, stirred for ½ hour. After that, we added an amount of NaOH to ajustate the pHat 10. Then, the mixture wasstirred for 3 h. The sample was placed in a sand bath at 100 °C to remove the water. The obtained material was washed and filtred to eliminate undesirable impurities. Drying in Oven over night and calcination at 400 °C.

Monometallic supported TiO_2 are prepared according to the 10% in weight.

2.2 Photocatalytic degradation experiments

2.2.1 Photocatalytic degradation experiments

2.2.1.1 Sunlight effect The photocatalytic activity of as prepared catalysts CuO / TiO_2 and NiO / TiO_2 was evaluated for the degradation of malachite green dye. Different dye concentrations (20–40-60 mg/l) were prepared using the stock solution. The reaction suspension was prepared by adding different amounts (0.1- 0.2- 0.3 g/l) of photocatalyst powder. Sunlight is used as sources irradiation in the photo degradation experiments.

The experiments were carried out during the months of May–June-July 2019 between 12 p.m. and 4 p.m. Skikda city North East of Algeria.

2.2.1.2 Effect of microwave power In an Erlenmeyer flask, we put 200 ml of a solution of 20 ml / g in malachite green. The tests were carried out without catalyst and in the presence of 0.1 g of catalyst. Then 1 ml of hydrogen peroxide is added. The tests were carried out in the microwave at (350 W) and (500 W). Synthesized catalysts are characterized using infrared spectroscopy to determine functional groups (Table 1).

2.3 Characterization of catalysts

2.3.1 Infrared spectroscopic analysis (FTIR)

FTIR spectra were performed using a "Perkin-Elmer Fourier Transform 1720-x" spectrometer, over a range of 400 to 4000 cm^{-1} with a resolution of 2 cm^{-1}.

Table 1 Kinetic constants for first-order reactions for different microwave powers

	C = 20 mg/l		C = 40 mg/l		C = 60 mg/l	
Catalyst	k_1	R_1^2	k_2	R_2^2	k_3	R_3^2
Ni/TiO_2	0.010	0.991	0.010	0.934	0.010	0.952
Cu/TiO_2	0.022	0.978	0.028	0.934	0.019	0.996
TiO_2	0.007	0.977	0.010	0.934	0.010	0.998

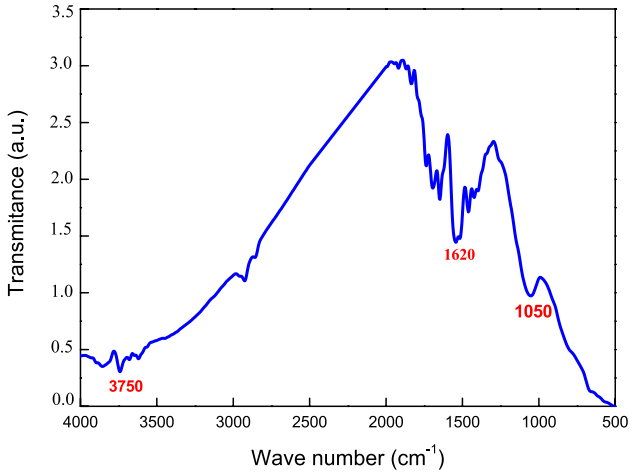

Fig. 1 IR spectrum of CuO/TiO_2

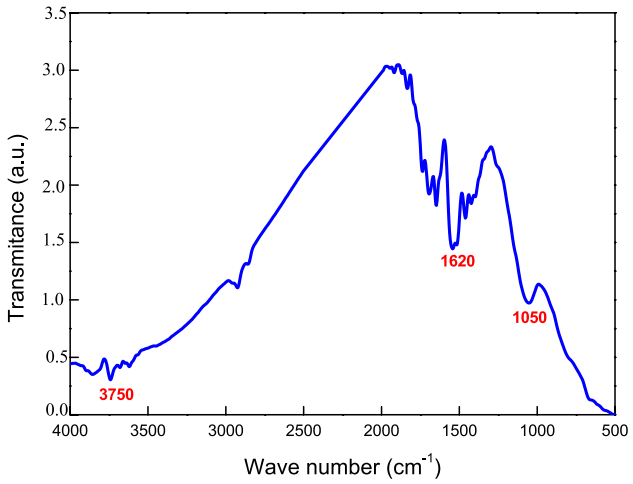

Fig. 2 IR spectrum of NiO/TiO_2

The results obtained in Figs. 1 and 2 show that all IR spectrum reveal the existence of the following essential bands:

The band in the range 3775–3600 cm^{-1}, with an intense peak at 3750 cm^{-1}, corresponds to the elongation vibrations of the O–H group binding.

A band appearing between 1629 and 1320 cm^{-1} that could be attributed to the valence vibrations (elongation) of the O–H bond of the constituent water and to the deformation vibrations of the bonds of the water molecules adsorbed in the pores.

A band between 1090 and 800 cm^{-1} corresponding to the vibration of the O-M–O and M–O-M bonds (M = Ni, Cu and Ti) in the structure of the solid.

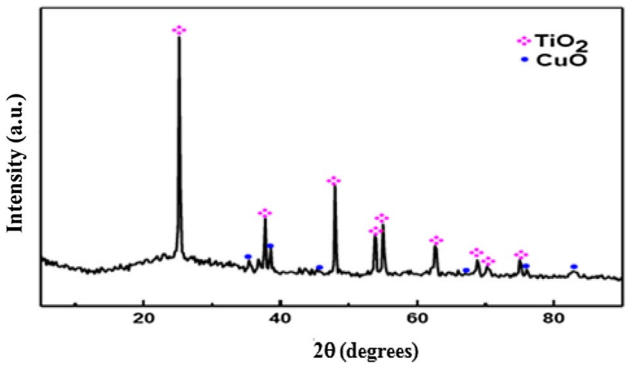

Fig. 3 X-ray diffraction spectra of CuO / TiO_2

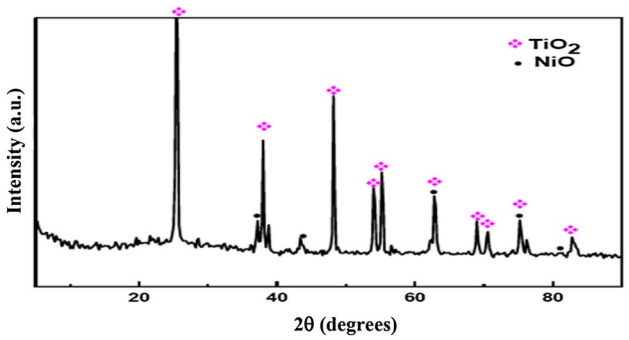

Fig. 4 X-ray diffraction spectra of NiO /TiO_2

There is also no band between 3500 and 3120 cm^{-1} corresponding to the vibrations of surface hydroxyl groups, this band being characterized by uncalcined solids.

2.3.2 X-ray diffraction analysis (XRD)

X-ray diffraction technique was performed to identify phase formation and crystallographic information of the samples. The XDR patterns of CuO/TiO_2, and NiO/TiO_2 (Figs. 3, 4 respectively), were carried out by the XPERT-PRO diffractometer type with Cu K_α radiation ($\lambda = 0.15406$ nm) and scanning over the 2θ range from 10 to 85°. The pattern exhibits a narrow diffraction peaks which is due to the well crystallization. According to JCPDS data, the peaks at 25.24, 38.10, 48.17, 53.81, 55.09, 62.6, 68.46 and 70.16° (JCPDS N° 84–1285) respectively are the characteristic reflections for anatase TiO_2 with structure tetragonal. However, The Presence of other peaks indicated the formation of metal oxide phases CuO (Fig. 3) (JCPDS No 89-5899) and NiO (Fig. 4) (JCPDS No 73-1519).

3 Results and discussion

3.1 Photocatalytic degradation under solar irradiation

3.1.1 Effect of the initial concentration of malachite green

The photocatalytic activity of as prepared catalyst CuO/TiO_2 and NiO/TiO_2 was evaluated for the degradation of malachite green dye concentration. Figure 5 shows the photocatalytic degradation of malachite green at different initial concentration in the range from 20 to 80 mg/l.

The curves show that the rate of degradation increased with time at diverse initial concentrations. The results obtained show that the degradation of GM solutions is faster in the presence than in the absence of catalyst. It was also noted that CuO/TiO_2 catalyst gives better results than NiO/TiO_2 and TiO_2 catalyst for all concentrations. The decolorization efficiency decreased with the increasing concentration which is possibly due to the difficulty of penetration of UV irradiations into a large concentration gradient. Then, it can be due to the adsorption of molecular dyes on the catalyst surface occupying the active sites (Mishra et al. 2015).

3.1.2 Effect of catalyst dosage

To optimize the dose of the photocatalyst, the photocatalytic degradation kinetics of malachite green is performed for different catalyst amount (0.1, 0.2, 0.3 g/l).

The results obtained and plotted in Fig. 6 show that the mass of the catalyst has a very significant effect on the dye degradation. It has been noted that the C_t/C_0 ratio decreases more rapidly over time in the presence of different catalyst masses and that the best result is obtained with 0.3 g of CuO /TiO_2 catalyst.

The particles of catalysts that are semiconductors are at the origin of this activation. They will absorb solar radiation to give rise to highly reactive species that will lead to the degradation of the dye in solution. The degradation efficiency increase as the catalyst dose increase, due to the increase of the active sites on the catalyst surface. The CuO/TiO_2, NiO/TiO_2 photocatalyst show a higher activity than the TiO_2 this can be explained by the fact that TiO_2 GAP has decreased by doping copper and nickel. According to literature, we can give the explanation below (Fig. 7).

Heterogeneous photo catalysis process can be divided into five independent steps (Eskandarloo et al. 2015):

1. Transfer of reagents from the liquid phase at the photocatalyst surface

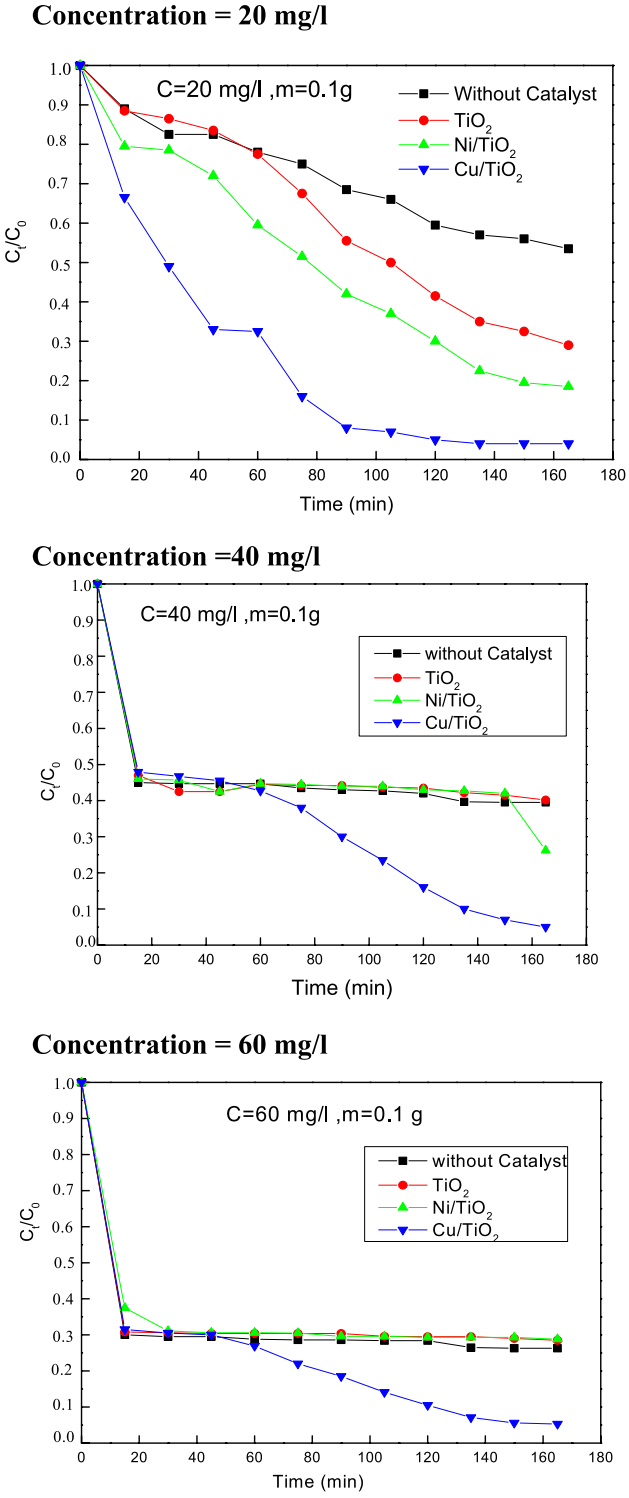

Fig. 5 Influence of catalyst concentrations on the kinetic curves for the degradation of the GM solutions resulting from heterogeneous Photocatalytic reactions under visible light

2. Adsorption of reagent on the photocatalyst surface
3. Photocatalytic reaction in adsorbed phase
4. Desorption of product (s)
5. Removal of products.

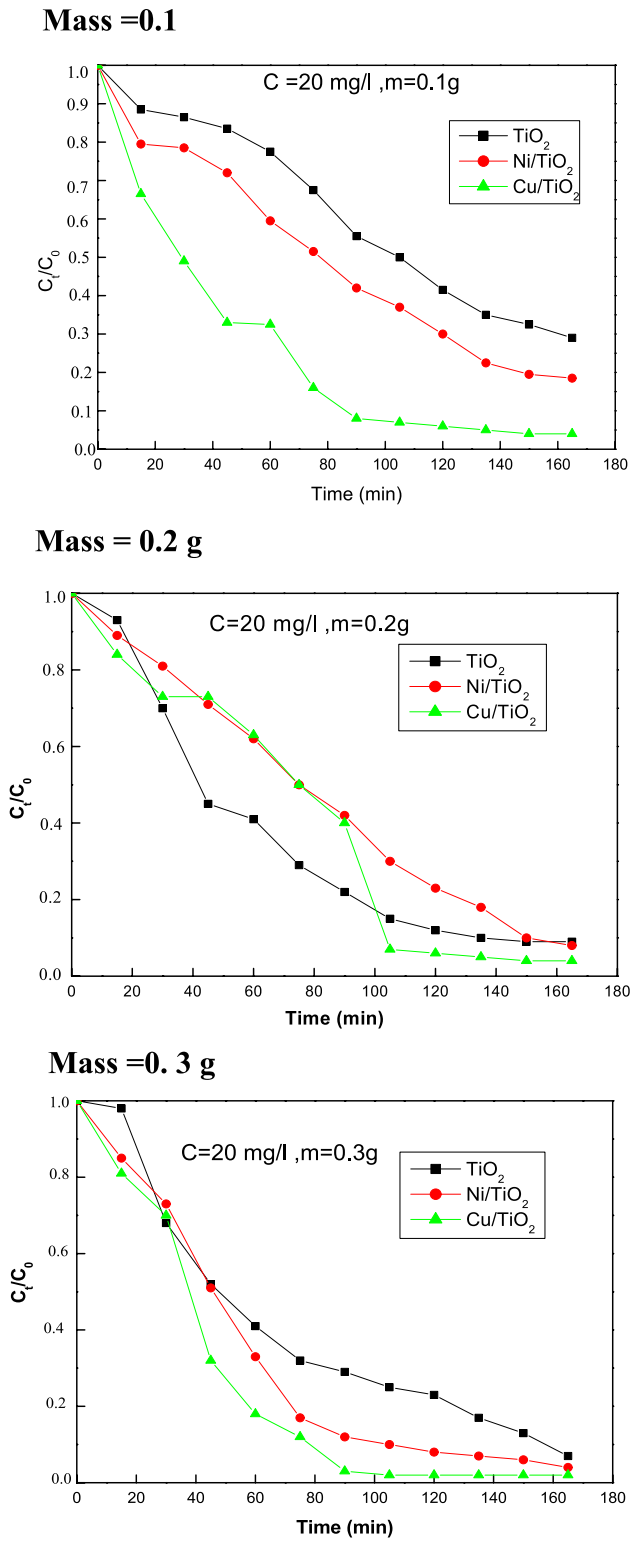

Fig. 6 Influence of catalyst dose on the kinetic curves for the degradation of the GM solutions resulting from heterogeneous Photocatalytic reactions under visible light

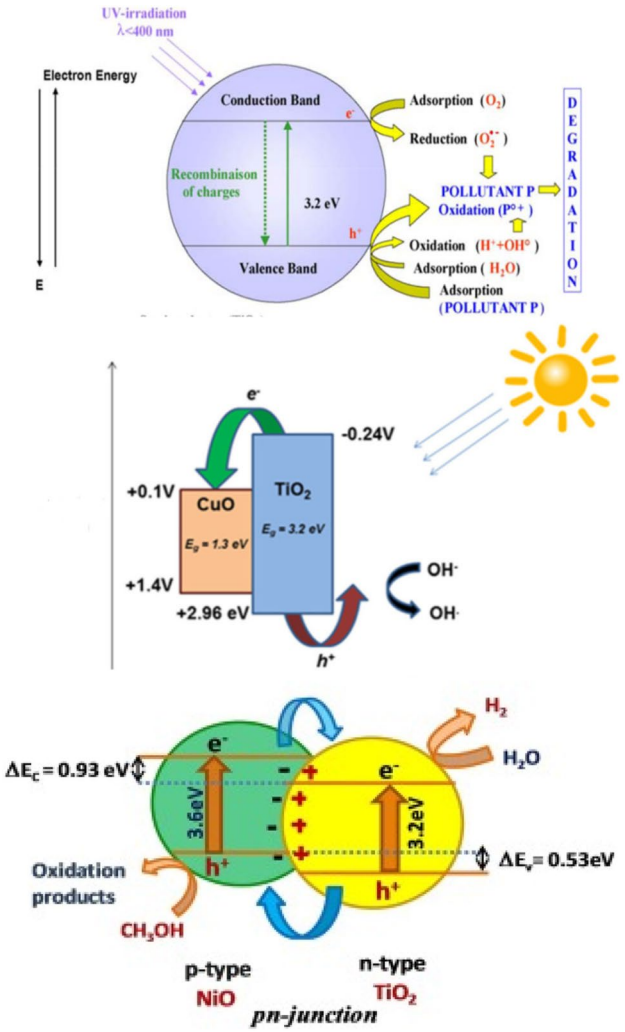

Fig. 7 Schematic diagram illustrating the principle of TiO_2, CuO/TiO_2 and NiO/TiO_2 Photo catalysis [[21], Janczarek et al. 2017, Arana et al. 2008, Marcin et alsss. 2017]

Reactions:

$$TiO_2 + h\nu \rightarrow TiO_2(e^- + h^+) \quad (1)$$

The electrons in the metal's conduction band can reduce dissolved oxygen with the formation of radical superoxide ion O_2^-

Molecular oxygenacts as an electron acceptor in the transfer reaction [25]

$$TiO_2(e) + O_2 \rightarrow O_2^{\cdot -} \quad (2)$$

The radical superoxide ion $O_2^{\cdot -}$ reactwithH_2O to give $HO^{\cdot}$, OH^- et O_2

$$2O_2^{\cdot -} + 2H_2O \rightarrow H_2O_2 + 2OH^- + O_2 \quad (3)$$

The photocatalysis of hydrogenperoxide regenerates the free hydroxyl radical $OH^{\cdot}$

$$2H_2O_2 + TiO_2(e) \rightarrow OH^- + HO^{\cdot} \quad (4)$$

$$O_2^{\cdot -} + 2H^+ \rightarrow 2HO_2^{\cdot} \quad (5)$$

While the h^+ (positive holes) react with the adsorbed H_2O or OH^-, thus giving an $OH^{\cdot}$ radical, according to the reactions(Eqs. 5 and 7), we can also witness direct oxidation by electron transfer from the adsorbed substrate (pollutant) on the surface depending on the reaction(Eq. 6) (Mungondori et al. 2013)

$$TiO_2(h^+) + H_2O_{abs} \rightarrow TiO_2 + OH^{\cdot}_{abs} + H^+ \quad (6)$$

$$TiO_2(h^+) + OH^-_{abs} \rightarrow TiO_2 + OH^{\cdot}_{abs} \quad (7)$$

$$TiO_2(h^+) + RX_{ads} \rightarrow TiO_2 + RX^{\cdot +}_{ads} \quad (8)$$

Direct Oxydation,

$$TiO_2(h^+) + R \rightarrow TiO_2 + R^{\cdot} \rightarrow \text{degradation products} \quad (9)$$

As an example of the last process, the hydroxyl radicals oxidize the C-H bond to give a carboxylic group which is decarboxylate according to Eq. 10.

$$RCOO^- + h^+ \rightarrow R^{\cdot} + CO_2 \quad (10)$$

The hydroxyl radicals formed, are also involved in the degradation of pollutants (RX)

$$OH^{\cdot} + RX \rightarrow CO_2 + H_2O \quad (11)$$

$$OH^{\cdot} + R \rightarrow R^{\cdot} + H_2O \quad (12)$$

The next step is of great importance, especially because of the high concentration of OH^-, due to the dissociation of water [25].

$$H_2O \rightarrow OH^- + H^+ \quad (13)$$

Much of the electron–hole pairs recombine in the particle volume or on the surface which reduces the quantum yield (Mungondori et al. 2013).

Whereas, considering the reduction potential for Cu^{2+}/Cu^+ (+0.17 V vs. NHE (normal hydrogen electrode) CuO dopped TiO_2 could react with the photogenerated electrons and Cu^+ ions could be re-oxidized to Cu^{2+} by oxygen, H_2O_2 or other oxidizing species present in the medium

$$Cu^{2+} + e^- CB \rightarrow Cu^+ \quad (14)$$

$$Cu^+ + (O_2, H_2O_2, \text{other oxidants}) \rightarrow Cu^{2+} + e^- \quad (15)$$

Therefore, the Reaction (14) of Cu^{2+} ions with the photo generated electrons should slow down electron-hole combination resulting in activity enhancement (Arana et al. 2008).

3.2 Photocatalytic degradation via microwave

3.2.1 Effect of microwave power

The influence of the microwave power in the degradation of green malachite was examinated for CuO/TIO_2, NiO/TiO_2 and TiO_2 catalysts under power of 350 W and 500 W.

The results obtained and plotted in Figs. 8, 9 show that the power of the microwave oven has a very significant effect on the degradation. It was noted that the C_t/C_0 ratio decreases rapidly over time. At 500 power, the two supported catalysts have almost the same efficiency. The CuO/TiO_2 catalyst has the best efficiency for GM degradation at 350 W power. However, we notice that TiO_2 has not a good reactivity via microwave. Indeed, when the power has increased from 350 to 500 W, the reaction in the absence of catalyst is more effective than that in the presence of TiO_2. This can be explained by the increase in combination reactions that inhibits the degradation reaction (Figs. 10, 11, 12, 13, 14, 15, 16, 17, 18, 19, 20, 21, 22, 23, 24, 25).

3.2.2 Kinetic study of the degradation reaction of malachite green

Kinetics study of removal of green malachite by photocatalytic degradation was investigated at different

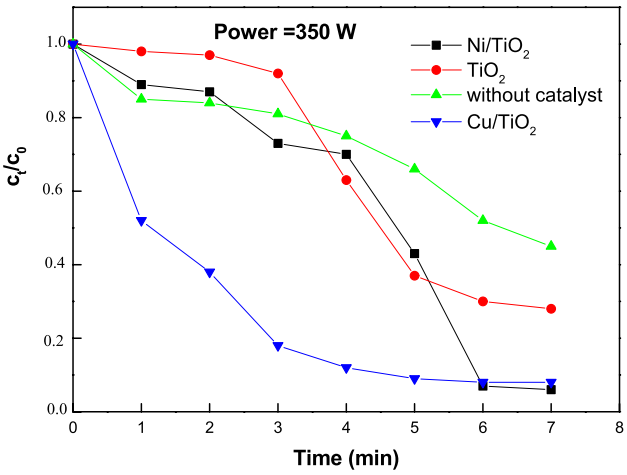

Fig. 8 Kinetic curves for the degradation of GM solutions resulting from photocatalytic reactions in the presence and the absence of catalysts under 350 W microwave oven power (20 mg/l; 1 ml H_2O_2)

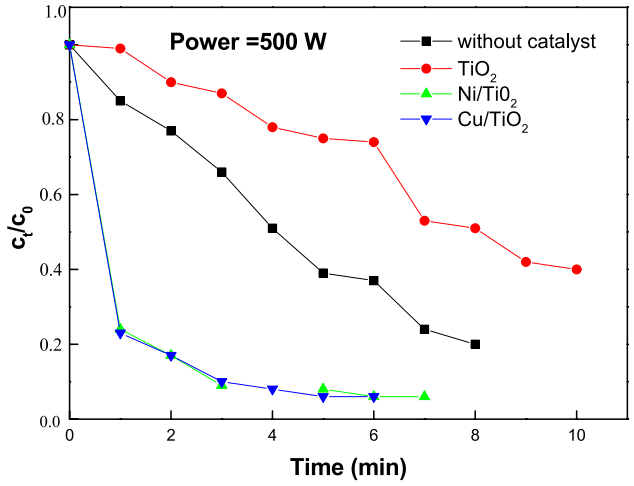

Fig. 9 Kinetic curves for the degradation of GM solutions resulting from photocatalytic reactions in the presence and the absence of catalysts under 500 W microwave oven power (20 mg/l; 1 ml H_2O_2)

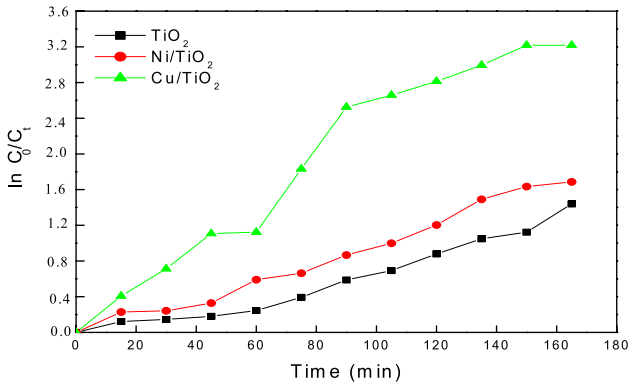

Fig. 10 First order Kinetics of dye degradation for various catalysts at 20 mg/l

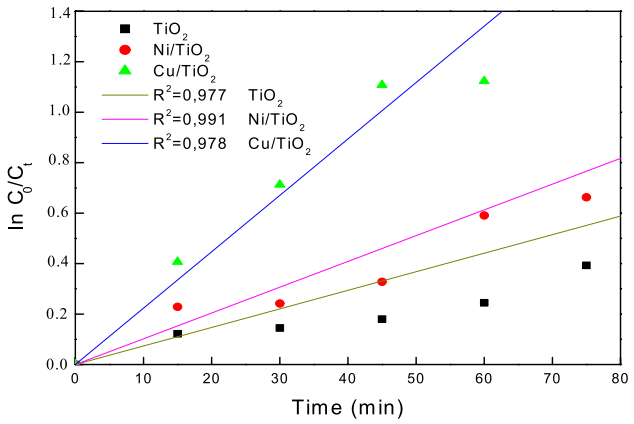

Fig. 11 First order Kinetics of dye degradation for various catalysts at 20 mg/l at the first time

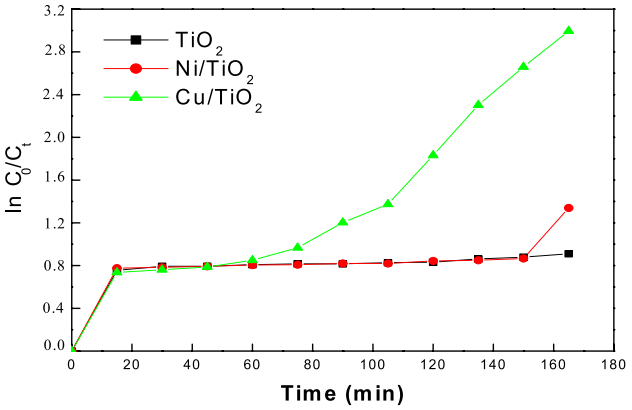

Fig. 12 First order Kinetics of dye degradation for various catalysts at 40 mg/l

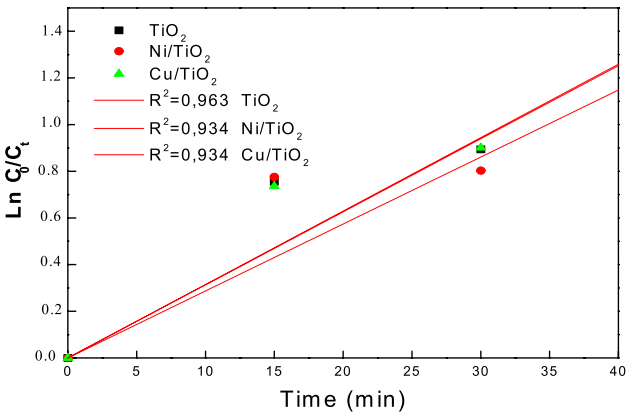

Fig. 13 First order Kinetics of dye degradation for various catalysts at 20 mg/l at the first time

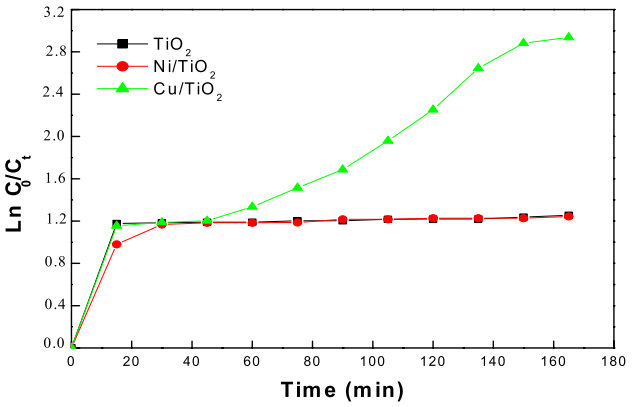

Fig. 14 First order Kinetics of dye degradation for various catalysts at 60 mg/l

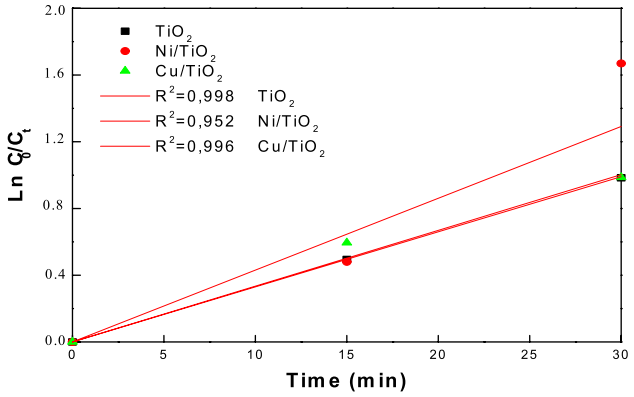

Fig. 15 First order Kinetics of dye degradation for various catalysts at 60 mg/l at the first time

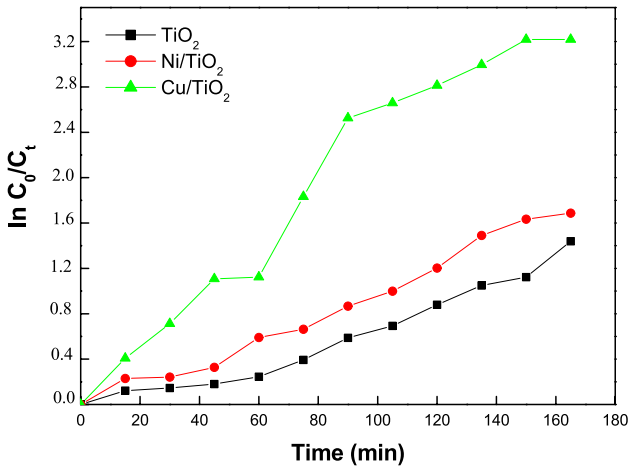

Fig. 16 First order Kinetics of dye degradation for 20 mg/l and a catalyst mass of 0.1 g

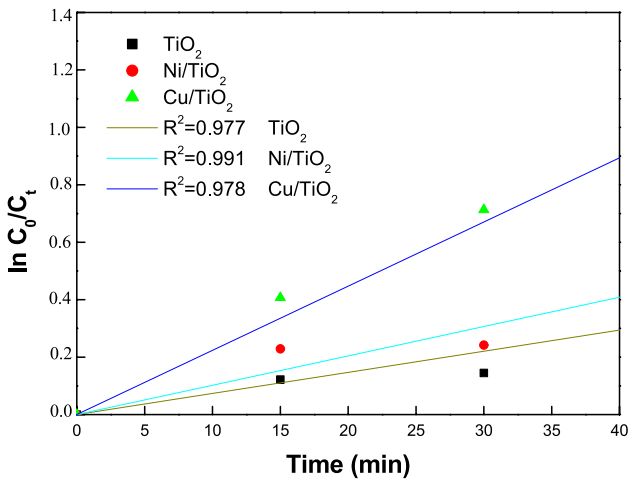

Fig. 17 First order Kinetics of dye degradation for 20 mg/l and a catalyst mass of 0.1 g at the first time

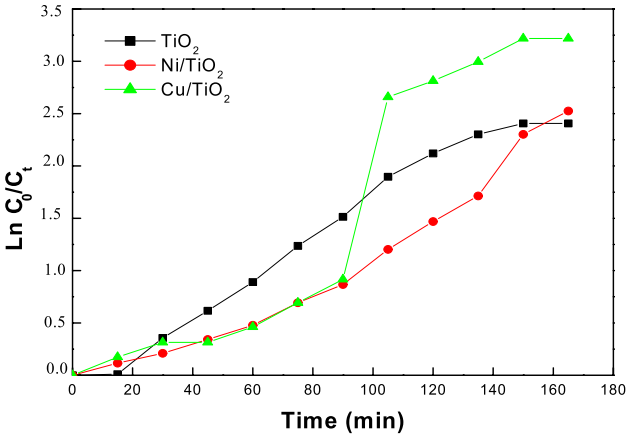

Fig. 18 First order Kinetics of dye degradation for 20 mg/l and a catalyst mass of 0.2 g

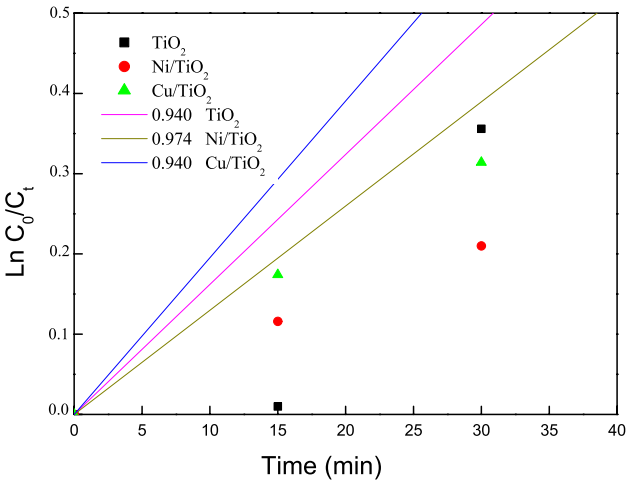

Fig. 19 First order Kinetics of dye degradation for 20 mg/l and a catalyst mass of 0.2 g at the first time

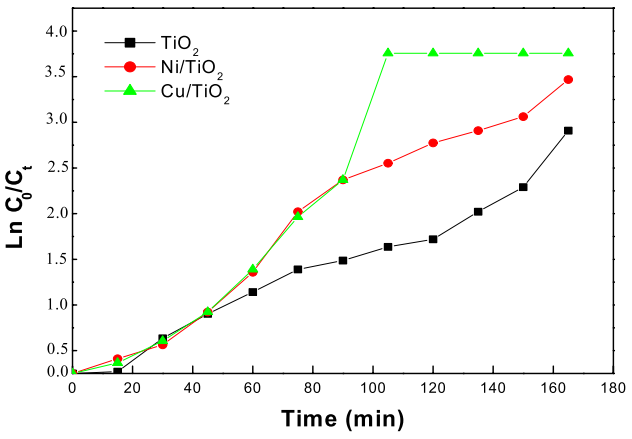

Fig. 20 First order Kinetics of dye degradation for 20 mg/l and a catalyst mass of 0.3 g

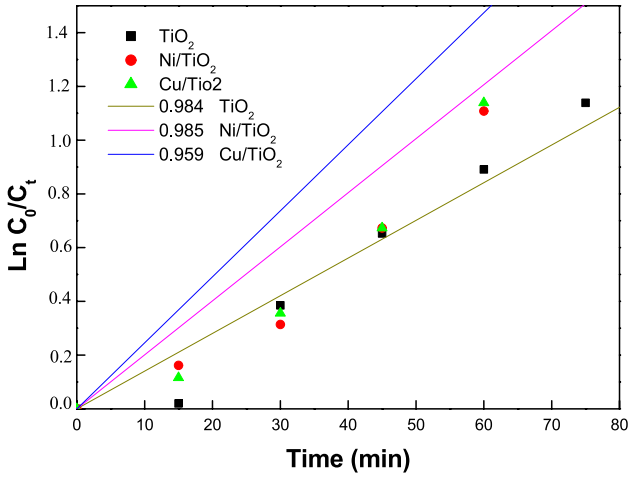

Fig. 21 First order Kinetics of dye degradation for 20 mg/l and a catalyst mass of 0.3 g at the first time

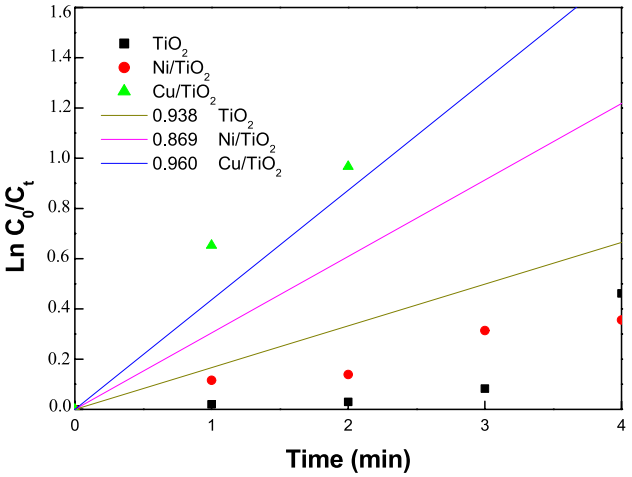

Fig. 23 First order Kinetics of dye degradation for 20 mg/l concentration and at 350 W microwave power at first time

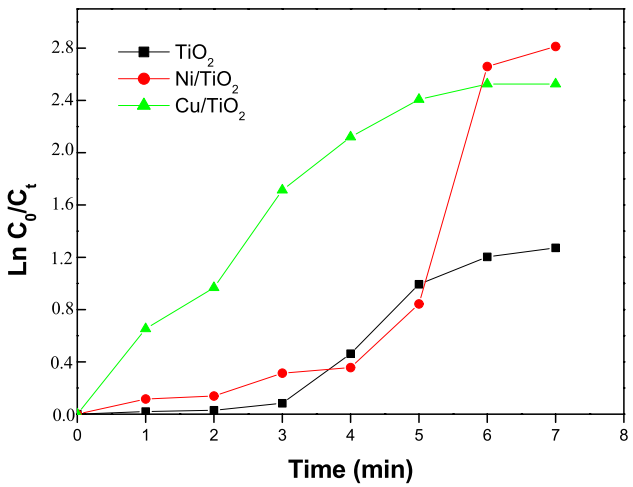

Fig. 22 First order Kinetics of dye degradation for 20 gm/l and at 350 W microwave

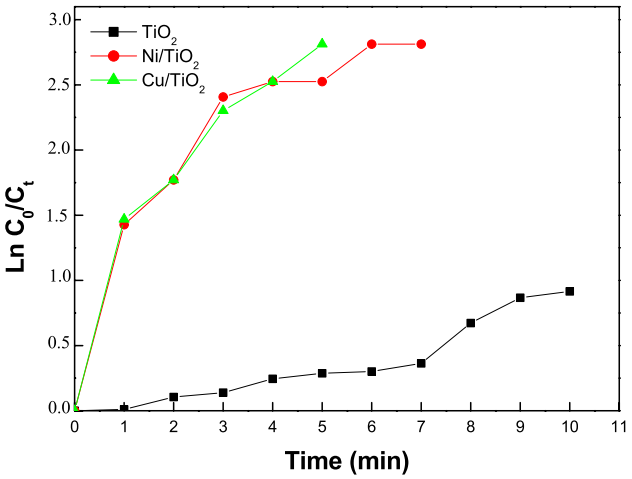

Fig. 24 First order Kinetics of dye degradation for 20 mg/l concentration and at 500 W microwave power

initial concentration, different dose of catalysts and different microwave power.

In the present work, pseudo first order kinetic model is used to find the rate of photodegradation of GM.

$$v = \frac{dc}{dt} = K_{app} C$$

$$\text{Ln } C_0/C_t = K_{app} t$$

where: v: photocatalytic degradation rate ($mg.l^{-1}.min^{-1}$). Kapp: apparent degradation constant (min^{-1}). C: concentration (mg./l). T: irradiation time (min).

3.2.3 Kinetics of different concentrations of GM

The plot of Ln (C_0/C_t) against time gives the apparent rate constant Kapp obtained from the slope. The figures show that the mineralization of GM in the presence of oxidizing agent (H_2O_2) with different catalysts follows a first order kinetics for all concentrations (20, 40, 60 mg/l) in the photocatalytic application. The rate constants and correlation coefficients have calculated and presented in Tables 2 and 3. Correlation coefficients, which are above 0.9 for degradation of GM in the presence of different catalysts and for different concentrations follows the first order kinetics. The highest rate constant was observed for CuO/TiO_2 cataltyst: Kapp CuO/TiO_2 > Kapp NiO/TiO_2 > Kapp TiO_2. This result mainly because of the synergetic effect of narrow band

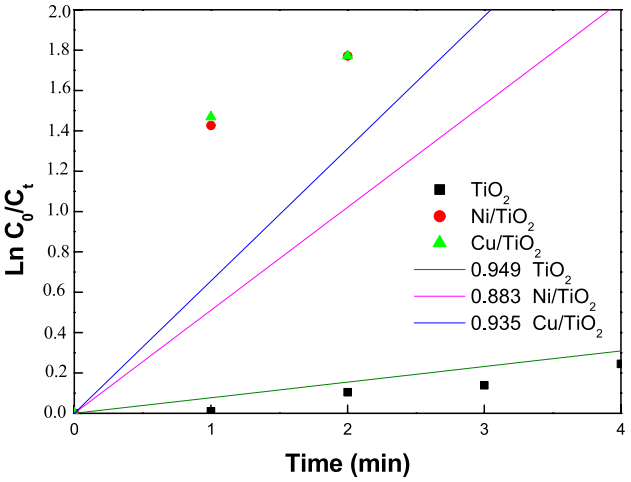

Fig. 25 First order Kinetics of dye degradation for 20 mg/l concentration and at 500 W microwave power at the first time

gab in the visible light range which hinder the recombination of generated electron–hole pairs (Wei et al. 2018).

3.2.4 Kinetics of the different catalyst masses

3.3 Kinetics of catalysts with different microwave powers

The results obtained in the table and previous figures show that the photocatalytic degradation of the GM in the presence of the oxidizing agent (H_2O_2) and different microwave powers follows first-order kinetics for all the solutions. The value of the rate constant K_{app} increase with power increase from 0.304 to 0.510 for NiO/TiO_2 and from 0.435 to 0.656 for CuO/TiO_2, whereas for TiO_2 catalyst the rate constant decrease. Kapp of CuO/TiO_2 is higher than that of NiO/TiO_2. The rate constant K_{app} at microwave power are very highest at the rate constant at sun light.

4 Conclusion

In this work, supported nickel-copper catalysts were synthesized on titanium dioxide by the liquid or "wet" diffusional impregnation process.

These catalysts are tested to remove malachite green (GM), which is a synthetic dye present in textile and tanning industry effluents by the advanced oxidation process (AOP) in the presence of hydrogen peroxide and catalysts under solar and microwave irradiation.

The results show that Malachite green is easily removed with the advanced oxidation process. Mass and concentration are important factors in the study of dye photo-degradation. The photo-degradation reaction via microwave is faster than that via solar irradiation.

Infrared (IR) spectrometric analysis revealed the presence of M–O or M–O-M oxide characteristic bands (M = Ni or Cu), and the absence of strange species or surface hydroxyl groups (bound OH). The DRX spectra of our solids have made it possible to identify the different crystalline phases present, such as CuO, NiO and TiO_2 supports.

Table 2 Kinetic constants for first-order reactions for different concentrations

	m = 0.1 g		m = 0.2 g		m = 0.3 g	
Catalyst	k_1	R_1^2	k_2	R_2^2	k_3	R_3^2
Ni/TiO_2	0.010	0.991	0.012	0.974	0.020	0.985
Cu/TiO_2	0.022	0.978	0.019	0 .940	0.024	0.959
TiO_2	0.007	0.977	0.012	0 .940	0.014	0.984

Table 3 Kinetic constants for first-order reactions for different masses

	Power = 350 W		Power = 500 W	
Catalyst	k_1	R_1^2	k_2	R_2^2
Ni/TiO_2	0.304	0.869	0.510	0.883
Cu/TiO_2	0.435	0.960	0.656	0 .935
TiO_2	0.166	0.938	0.077	0 .949

Compliance with ethical standards

Conflict of interest The author(s) declare that they have no competing interests.

References

1. Flox C, Ammar S, Arias C, Brillas E, Vargas-Zavala AV, Abdelhedi R (2006) Electro-Fenton and photoelectro-Fenton degradation of indigo Carmine in acidic aqueous medium. Appl Catal B Environ 67:93–104
2. Ji F, Li C, Zhang J, Deng L (2011) J Hazard Mater 186:1979–1984
3. Gauthier H, Yargeau V, Gooper DG (2010) Biodegradation of pharmaceuticals by *Rhococcusrhodochrous* and *Aspergillusniger* by co-metabolism. Sci Total Environ 408:1701–1706
4. Huang H, Leung DYC, Kwong PCW, Xiong J, Zhang L (2013) Catal Today 201:189–194
5. Eskandarloo H, Badiei A Photocatalytic application of Titania nanoparticles for degradation of organic pollutants. Nanotechnol Opt Sens 108–132
6. Mungondori HH, Tichagwa L (2013) Photo-catalytic activity of carbon/nitrogen doped TiO_2-SiO_2under UV and visible light irradiation. Mater Sci Forum 734:226–236
7. Zhang J, Lee KH, Cui L, Jeong TS (2009) J Ind Eng Chem 15:185–189
8. Dutta K, Mukhopadhyaya S, Bhattacharjee S, Chaudhuri B (2001) Chemical oxidation of methylene blue using a Fenton-like reaction. J Hazard Mater B 84:57–71
9. Uddin MT, Islam MA, Mahmud S, Rukanuzzaman M (2009) Adsorptive removal of methylene blue by tea waste. J Hazard Mater 164:53–60
10. Rafatullaha M, Sulaimana O, Hashima R, Ahmad A (2010) Adsorption of methylene blue on low-cost adsorbents: a review. J Hazard Mater 177:70–80
11. Zhu MX, Wang Z, Zhou LY (2008) J Hazard Mater 150:37–45
12. Elahifard MR, Ahmadvand S, Mirzanejad A (2018) Effects of Ni-doping on the photo-catalytic activity of TiO_2 anatase and rutile: simulation and experiment. Mater Sci Semicond Process 84:10–16
13. Vega MPB, Hinojosa-Reyes M, Hernández-Ramírez A, Mar JLG, RodríguezGonzález V, Hinojosa-Reyes L (2018) Visible light photocatalyticactivity of sol–gel Nidoped TiO_2 on p-arsanilic acid degradation. J Sol Gel Sci Technol
14. Haque MM, Raza W, Khan A, Muneer M (2014) Heterogeneous photocatalyzed degradation of barbituric acid and matrinidazoleunder visible light induced Ni, Mn, Mo and La-doped TiO_2. J Nanoeng Nanomanuf 4:135–139
15. Khan MM, Ansari SA, Pradhan D, Ansari MO, Hung Han D, Leeaand J, Hwan Cho M (2014) Band gap engineered TiO_2 nanoparticles for visible light induced photo electrochemical and photo catalytic studies. J Mater Chem A 2:637
16. Mishra M, Chun D (2015) Fe_2O_3 as a photocatalytic material: a review. Appl Catal A Gen 498:126–141
17. Nasralla N, Yeganeh M, Astuti Y, Piticharoenphun S, Shahtahmasebi N, Kompany A, Karimipour M, Mendis BG, Pooltone NRJ, Šiller L (2013) Structural and spectroscopic study of Fe-doped TiO_2 nanoparticles prepared by sol–gel method. ScientiaIranica F 20(3):1018–1022
18. Janczarek M, Kowalska E (2017) Revie on the origin of enhanced photocatalytic activity of copper-modifiedtitania in the oxidative reaction systems. Catalysts 7:317
19. Gayathri P, Dorathi RPJ, Palanivelu K (2010) Ultrason Sonochem 17:566–571
20. Andreozzi R, Caprio V, Insola A, Marotta R (1999) Advanced oxidation process (AOP) for waterpurification and recovery. Catal Today 53:51–59
21. Thakur RS, Chaudhary R, Singh C (2010) Fundamentals and applications of the photocatalytic treatment for the removal of industrial organic pollutants and effects of operational parameters: a review. J Renew Sustain Energy 2:042701
22. Mohammadi S, Sohrabi M, NozadGolikand A, Fakhri A (2016) Preparation and characterization of zinc and copperco-doped WO3 nanoparticles: application in photocatalysis and photobiology. J Photochem Photobiol 161:217–221
23. Xu J, Ao Y, Fu D (2009) A novel Ce, C-co doped TiO_2 nanoparticles and its photocatalytica ctivity under visible light. Appl Surf Sci 256:884–888
24. Yao Y, Zhao C, Zhao M, Wang X (2013) J Hazard Mater 263(2):726–734
25. Zhang Y, Yuan C, Wang Q, Hoffmann MR, Zhang X, Nie J, Hu C, Chen S, Qiao J, Wang Q, Cong Y (2019) Photoelectrochemicalactivity of CdS/Ag/TiO_2 nanorod composites: degradation of nitrobenzene coupled with the concomitant production of molecular hydrogen. Electrochim Acta
26. Qingfeng Z, Yanfeng L, Gaobo Y, Furui H, Kai C, Dunchao X, Xinyu Z, Yuhong F, Jiacheng L (2017) Degradation kinetics of sodium alginate via sono-Fenton, photo-Fenton and sonophoto-Fenton methods in the presence of TiO_2 nanoparticles. Polym Degrad Stab 135:111–120